Supporting Information

Germanane Synthesis with Simultaneous Covalent Functionalization: Towards Highly Functionalized Fluorescent Germanane

Jiri Sturala,[a] Jan Luxa,[a] Stanislava Matějková,[b] Zdenek Sofer,[a,] Martin Pumera[a,c,d*]*

[a] Department of Inorganic Chemistry, University of Chemistry and Technology Prague, Technicka 5, 166 28 Prague 6, Czech Republic

[b] Institute of Organic Chemistry and Biochemistry ASCR v.v.i., Flemingovo nam. 2, 166 10 Prague 6, Czech Republic

[c] Department of Chemical and Biomolecular Engineering, Yonsei University, 50 Yonsei-ro, Seodaemun-gu, Seoul 03722, Korea

[d] Future Energy and Innovation Laboratory, Central European Institute of Technology, Brno University of Technology, Purkyňova 656/123, Brno, CZ-616 00, Czech Republic

Table of Contents

Characterization Methods

FT-IR spectroscopy

Fourier transform infrared spectroscopy (FTIR) measurements were performed on a iS50R FTIR spectrometer (Thermo Scientific, USA). The measurement was performed using DLaTGS detector and KBr beamsplitter in the range 4000 – 400 cm^{-1} at a resolution of 4 cm^{-1} on diamond ATR crystal (region from 2300 to 2000 cm^{-1} is not shown in the spectra because of diamond absorption). Ge_6H_6 sample was in KBr pellet made from 300 mg of KBr and 0.5 mg of the sample.

Raman spectroscopy

inVia Raman microscope (Renishaw, England) in backscattering geometry with CCD detector was used for Ra-man spectroscopy. DPSS Nd-YAG laser (532 nm, 50 mW) with applied power of 1% and 50× magnification objective. The spectra were referenced according to a laser peak position at 0 cm^{-1}, the spectrometer was referenced prior to the measurements by acquiring spectrum of silicon and referenced to 521 cm^{-1}. The samples were deposited on a metal plate as a powder and measured immediately after the deposition.

X-ray photoelectron spectroscopy

High resolution X-ray photoelectron spectroscopy (XPS) was performed using an ESCAProbeP spectrometer (Omicron Nanotechnology Ltd, Germany) with a monochromatic aluminum X-ray radiation source (1486.7 eV). Wide-scan surveys of all elements were performed, with subsequent high-resolution scans of the C 1s, O 1s, F 1s and Ge 2p or 3d. Relative sensitivity factors were used to evaluate the element ratios from the survey spectra. The

samples were placed on a conductive carrier made from a high purity gold surface on silicon. An electron gun was used to eliminate sample charging during measurement (1–5 V). The values are referenced to the gold peak at 84.0 eV or adventitious carbon peak at 284.8 eV.

HR-TEM

High resolution transmission electron microscopy (HR-TEM) was performed using an EFTEM Jeol 2200 FS microscope (Jeol, Japan). A 200 keV acceleration voltage was used for measurement. Elemental maps and EDS spectra were acquired with SDD detector X-MaxN 80 TS from Oxford Instruments (England). Sample preparation was attained by drop casting the suspension (1 mg mL^{-1} in water) on a TEM grid (Cu; 200 mesh; Formvar/carbon) and dried at 60 °C for 12 h.

SEM/EDX microscopy

The morphology was investigated using scanning electron microscopy (SEM) with a FEG electron source (Tescan Lyra dual beam microscope). Elemental composition and mapping were performed using an energy dispersive spectroscopy (EDS) analyzer (X-MaxN) with a 20 mm^2 SDD detector (Oxford instruments) and AZtecEnergy software. To conduct the measurements, the samples were placed on a carbon conductive tape. SEM and SEM-EDS measurements were carried out using a 10 kV electron beam.

Elemental combustion analysis

Combustible elemental analysis (CHNS-O) was performed using a PE 2400 Series II CHNS/O Analyzer (Perkin Elmer, USA). The instrument was used in CHN operating mode (the most

robust and interference-free mode) to convert the sample elements to simple gases (CO_2, H_2O and N_2). The PE 2400 analyzer automatically performed combustion, reduction, homogenization of product gases, separation and detection. An MX5 microbalance (Mettler Toledo) was used for precise weighing of the samples (1.5–2.5 mg per single sample analysis). Using this procedure, the accuracy of CHN determination is better than 0.30% abs. Internal calibration was performed using an *N*-fenyl urea.

For analysis of F, the sample is combusted by Schöniger method (i.e. in quartz Erlenmeyer flask in oxygen atmosphere). Formed F^- is determined potentiometrically by using ion-selective electrode.

Fluorescence measurements

The fluorescence measurement was performed using system Fluorolog Extreme (Horiba; France) equipped with Xe lamp (450 W) and double excitation monochromator. For the measurement of emission spectra was used monochromator iHR320 with CCD detector (with thermoelectrically cooled PMT detector). The excitation wavelength was determined based on 3D excitation/emission spectra. The emission spectra were acquired at wavelength with emission at maximum using PMT detector, both slits 2.5 nm and integration time 1 s. The spectra were then transformed to energy scale (eV) with the use of Jacobian conversion.[1]

DFT Calculations

The model compounds (**Scheme S1**) were optimized in Gaussian 16, rev B.01[2] to minimum, as confirmed by frequency calculation (having no imaginary frequency) using DFT functional CAM-B3LYP[3] and Def2-TZVP basis set. Ultrafinegrid option for higher DFT accuracy and

empirical dispersion[4] (GD3BJ) to take into account weak long distance interactions. The spectra are not scaled.

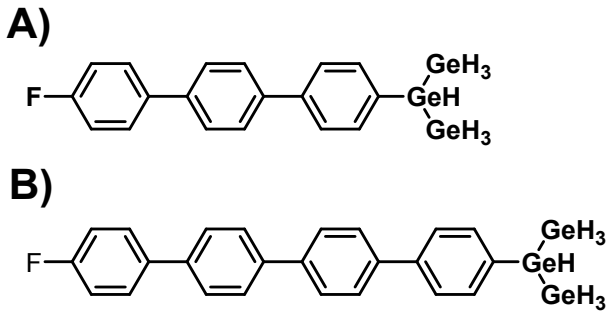

Scheme S1. Model compounds for calculation of Raman spectra. A) Ge_terphenyl; B) Ge_quaterphenyl.

Material Characterization

SEM/EDS

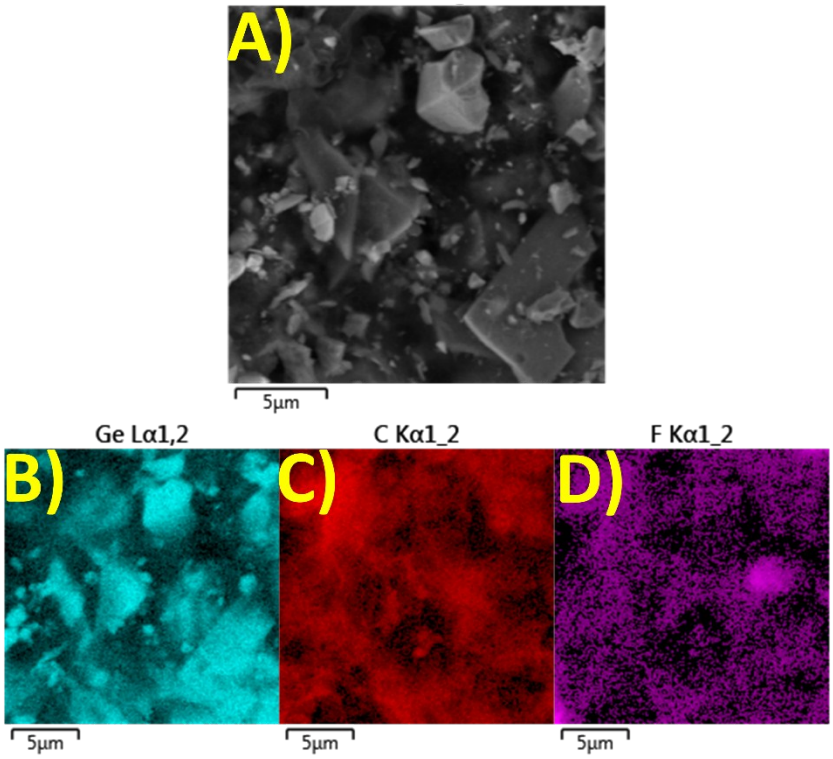

Figure S1. A) Electron image of modified germanane Ge_4FPh_I and corresponding EDS maps of individual elements (B) Ge, (C) C and (D) F.

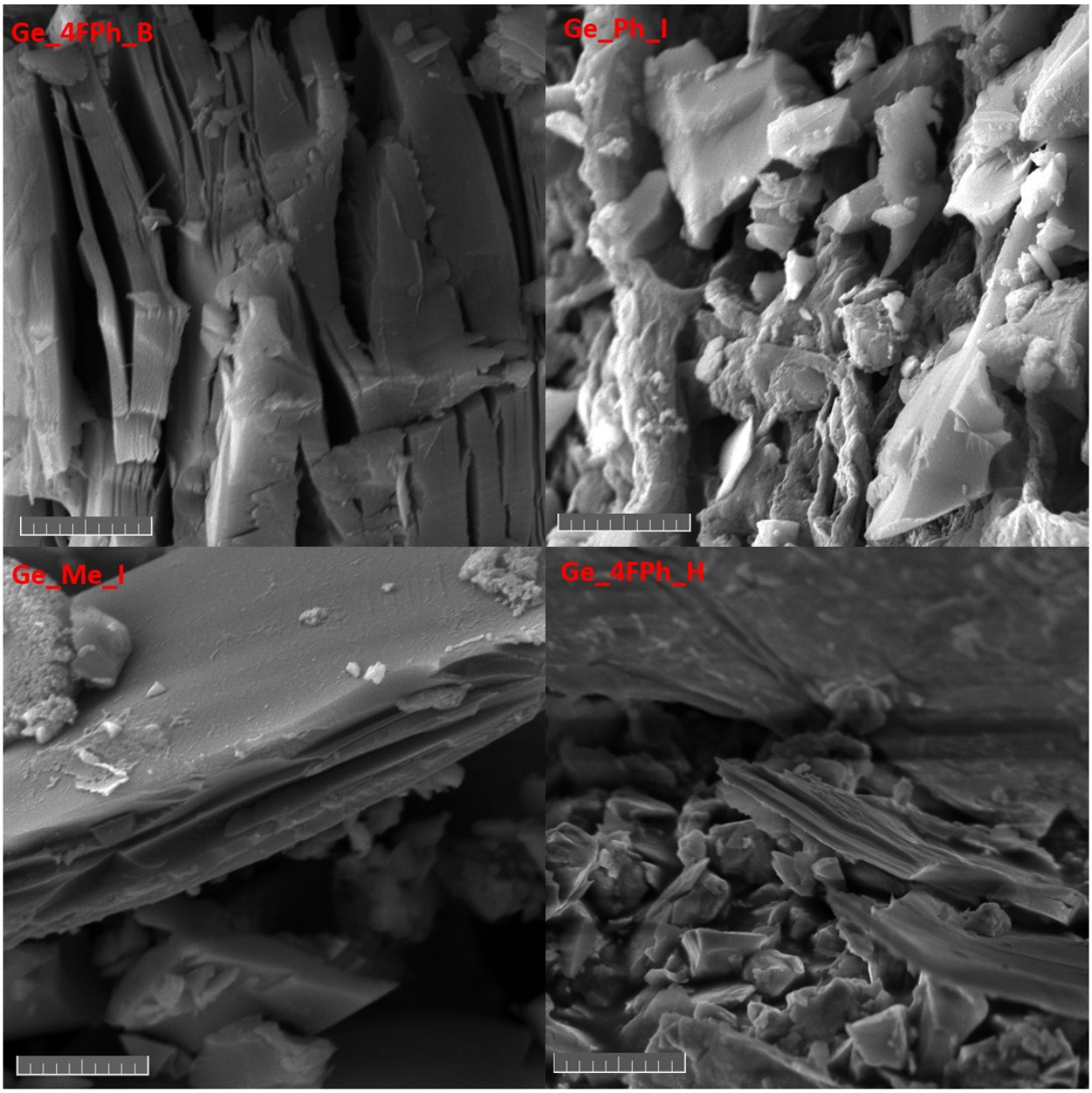

Figure S2. The morphology of germanene derivatives obtained by SEM. The scale bar corresponds to 2 μm.

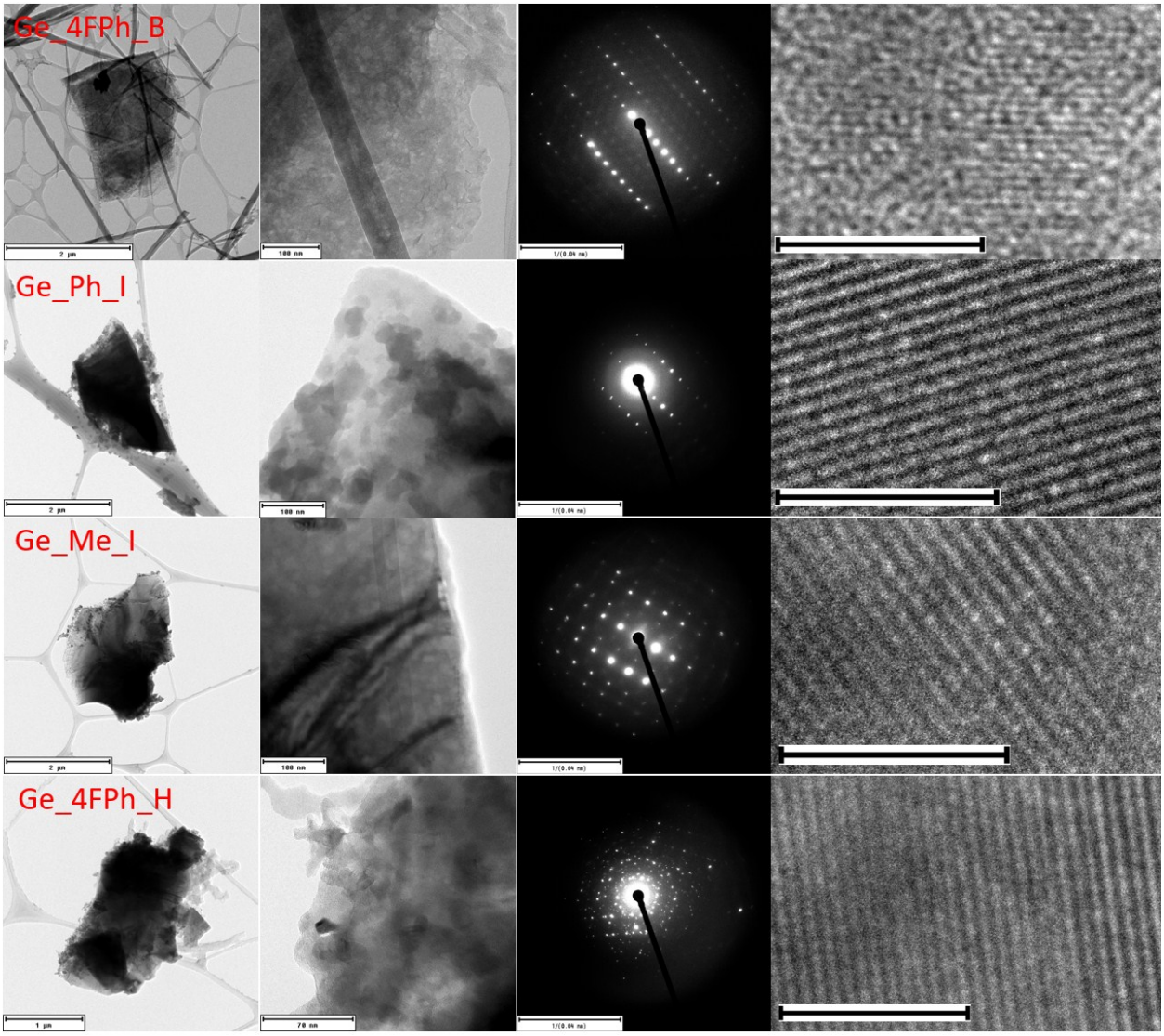

Figure S3. The TEM, SAED and HR-TEM images of exfoliated germanene samples. The scale bar on HR-TEM images correspond to 5 nm.

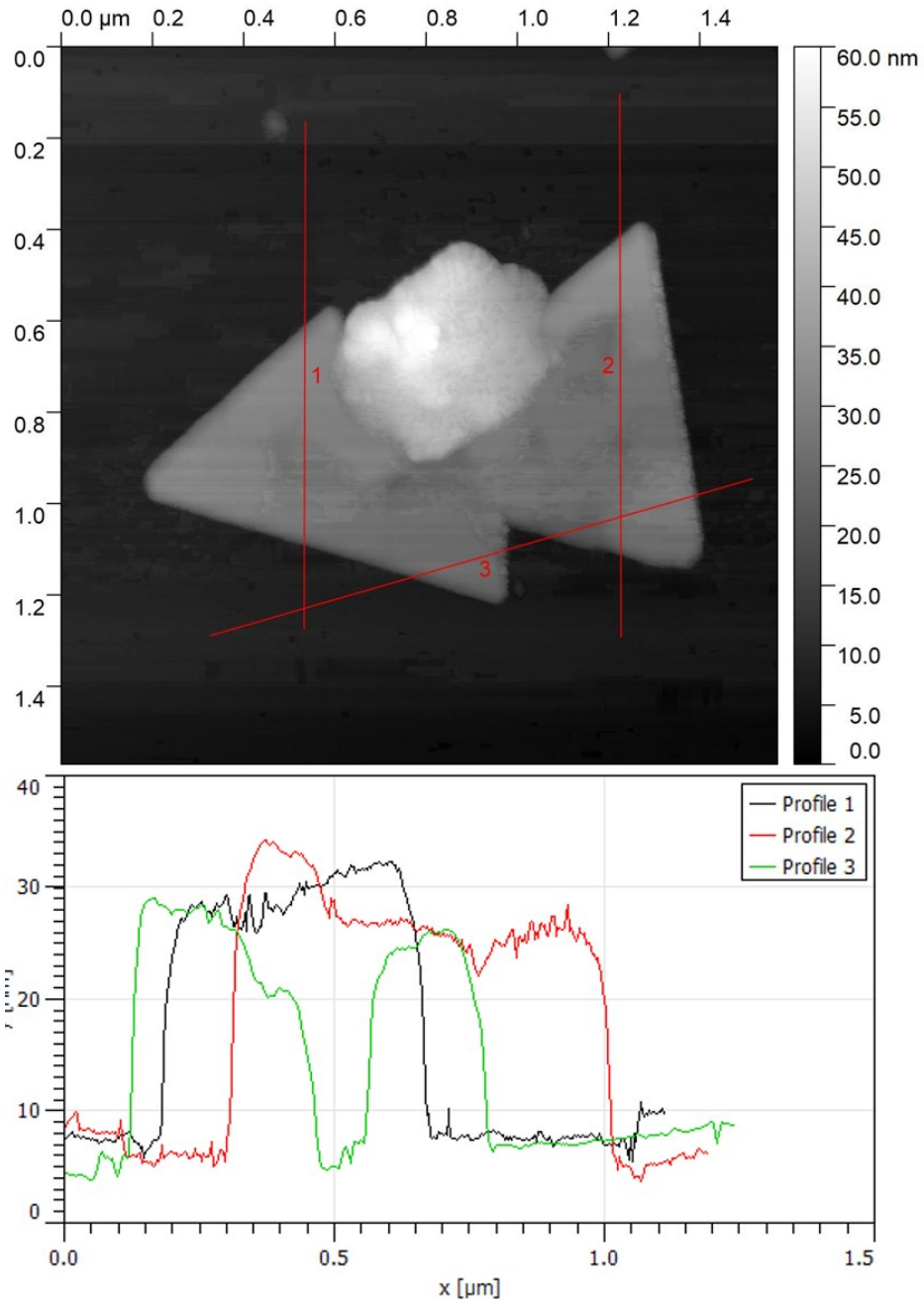

Figure S4. The AFM image of germanene sample Ge_4FPh_I and corresponding height profiles.

Elemental Combustion Analysis Results

Table S1. Elemental composition of the samples from combustion analysis in wt%.

Sample	C	H	N	F
$CaGe_2$	0.21	1.22	0.00	---[a]
Ge_6H_6	0.48	0.72	0.00	---[a]
Ge_4FPh_I	11.30	0.36	0.12	3.15
Ge_4FPh_H	2.49	0.55	0.00	0.57
Ge_4FPh_B	0.67	0.28	0.20	0.62
Ge_Ph_I	7.90	1.05	1.12	---[a]
Ge_Me_I	0.47	0.22	0.67	---[a]

[a] not measured.

FTIR spectra

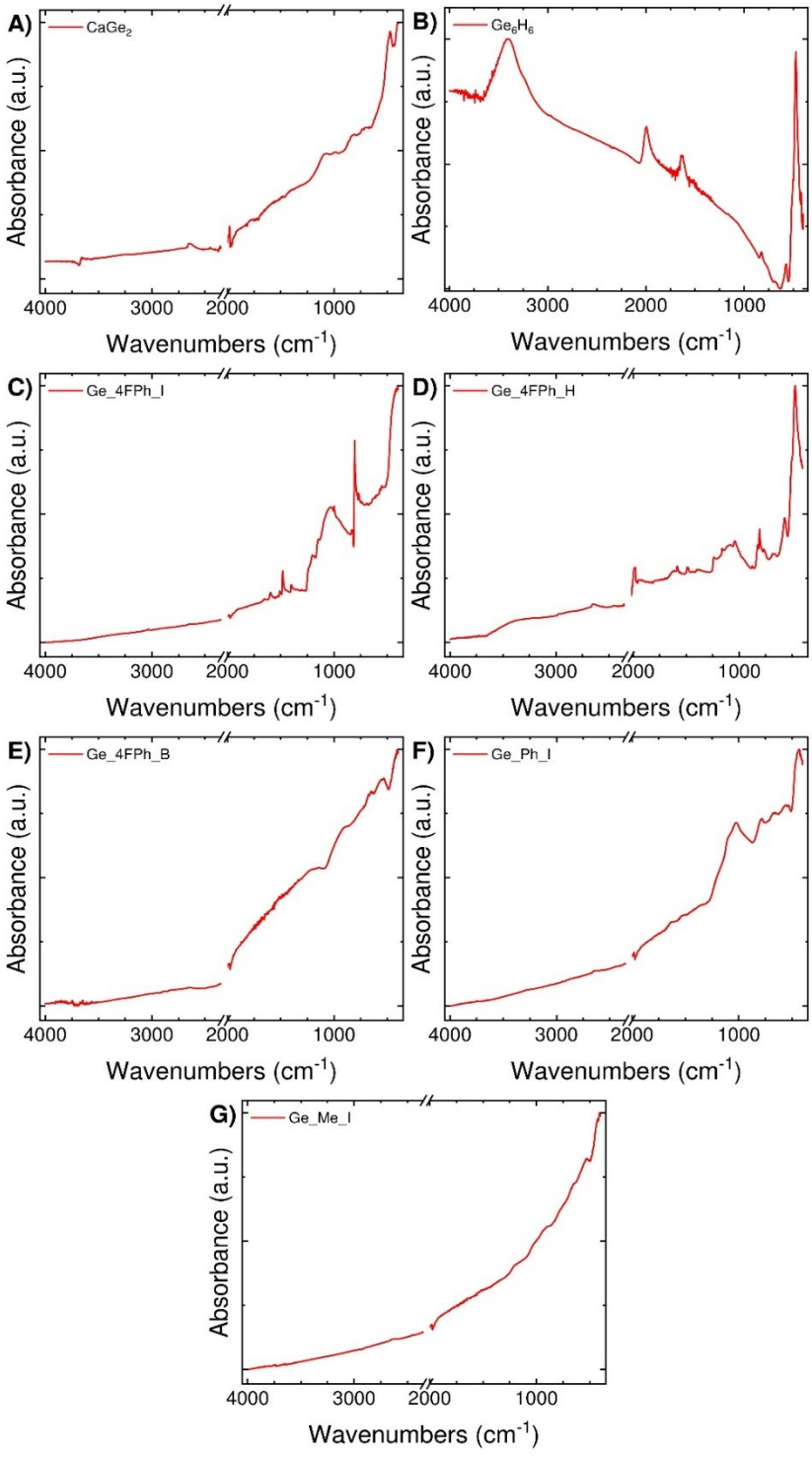

Figure S5. FTIR spectra of A) CaGe2, B) Ge6H6, C) Ge_4FPh_I, D) Ge_4FPh_H, E) Ge_4FPh_B, F) Ge_Ph_I, G) Ge_Me_I.

Raman Spectra

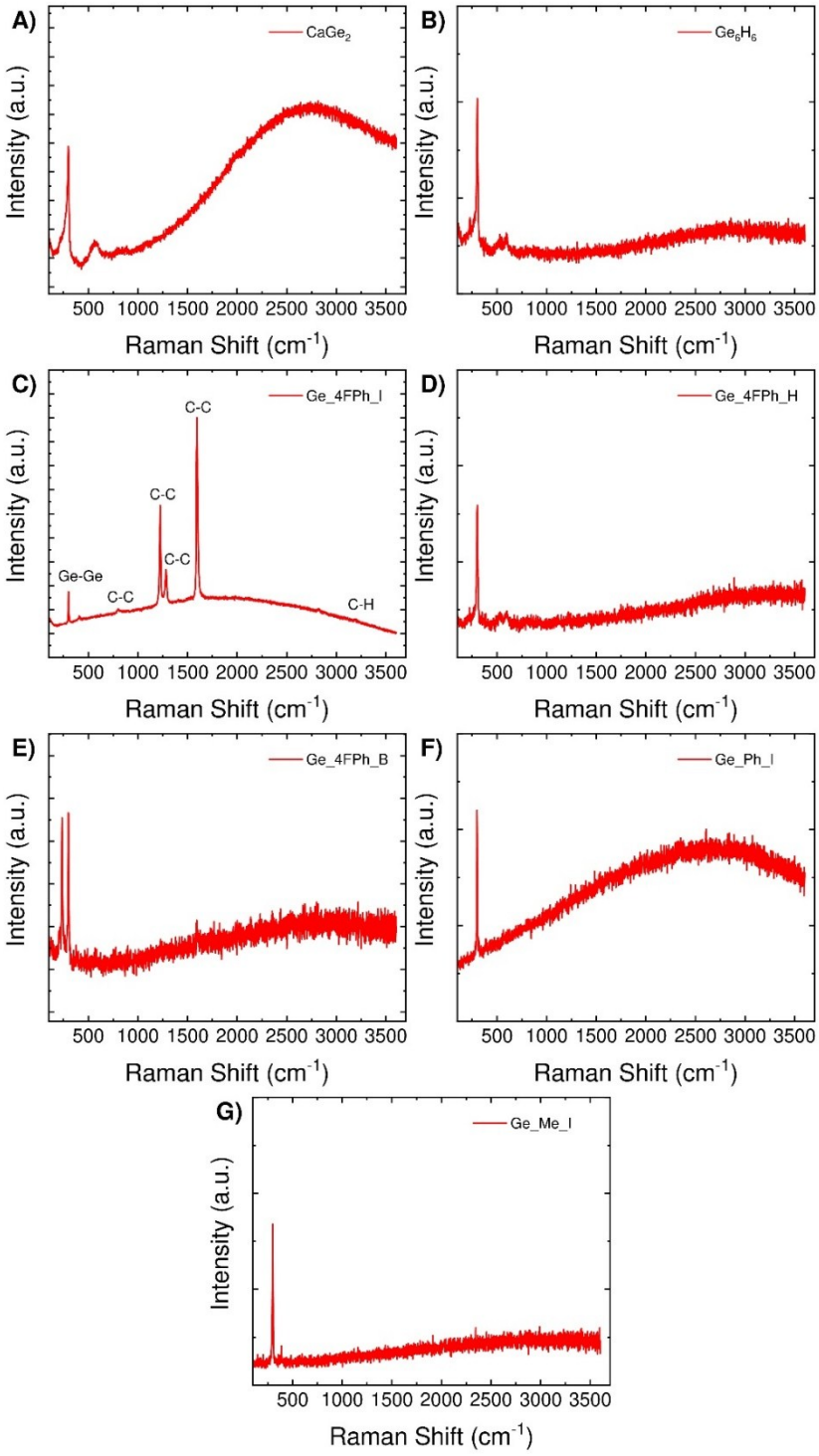

Figure S6. Raman spectra of A) $CaGe_2$, B) Ge_6H_6, C) Ge_4FPh_I, D) Ge_4FPh_H, E) Ge_4FPh_B, F) Ge_Ph_I, G) Ge_Me_I.

Predicted Raman Spectra

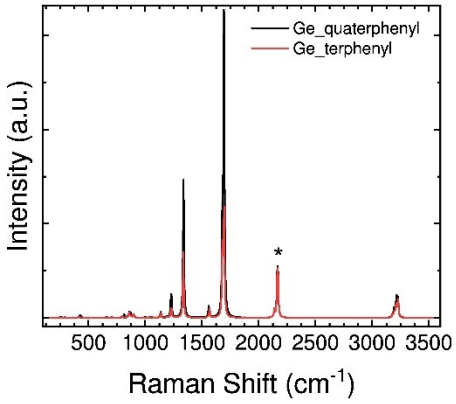

Figure S7. Predicted Raman spectra for Ge_p-fluoroquaterphenyl and Ge_p-fluoroterphenyl. Star labeled peak corresponds to Ge-H vibration.

3D excitation/emission spectra

Table S2. Excitation and Emission wavelengths/energies for modified germananes.

Sample	Excitation	Emission
$CaGe_2$	330 nm (3.76 eV)	530 nm (2.34 eV)
Ge_6H_6	310 nm (4.00 eV)	350 nm (3.54 eV)
Ge_4FPh_I	370 nm (3.35 eV)	430, 451, 480 nm (2.88, 2.75, 2.58 eV)
Ge_4FPh_H	370 nm (3.35 eV)	431, 456, 483 nm (2.88, 2.72, 2.57 eV)
Ge_4FPh_B	350 nm (3.54 eV)	430, 455, 486 nm (2.88, 2.72, 2.55 eV)
Ge_Ph_I	320 nm (3.87 eV)	494 nm (2.51 eV)
Ge_Me_I	325 nm (3.81 eV)	517 nm (2.40 eV)

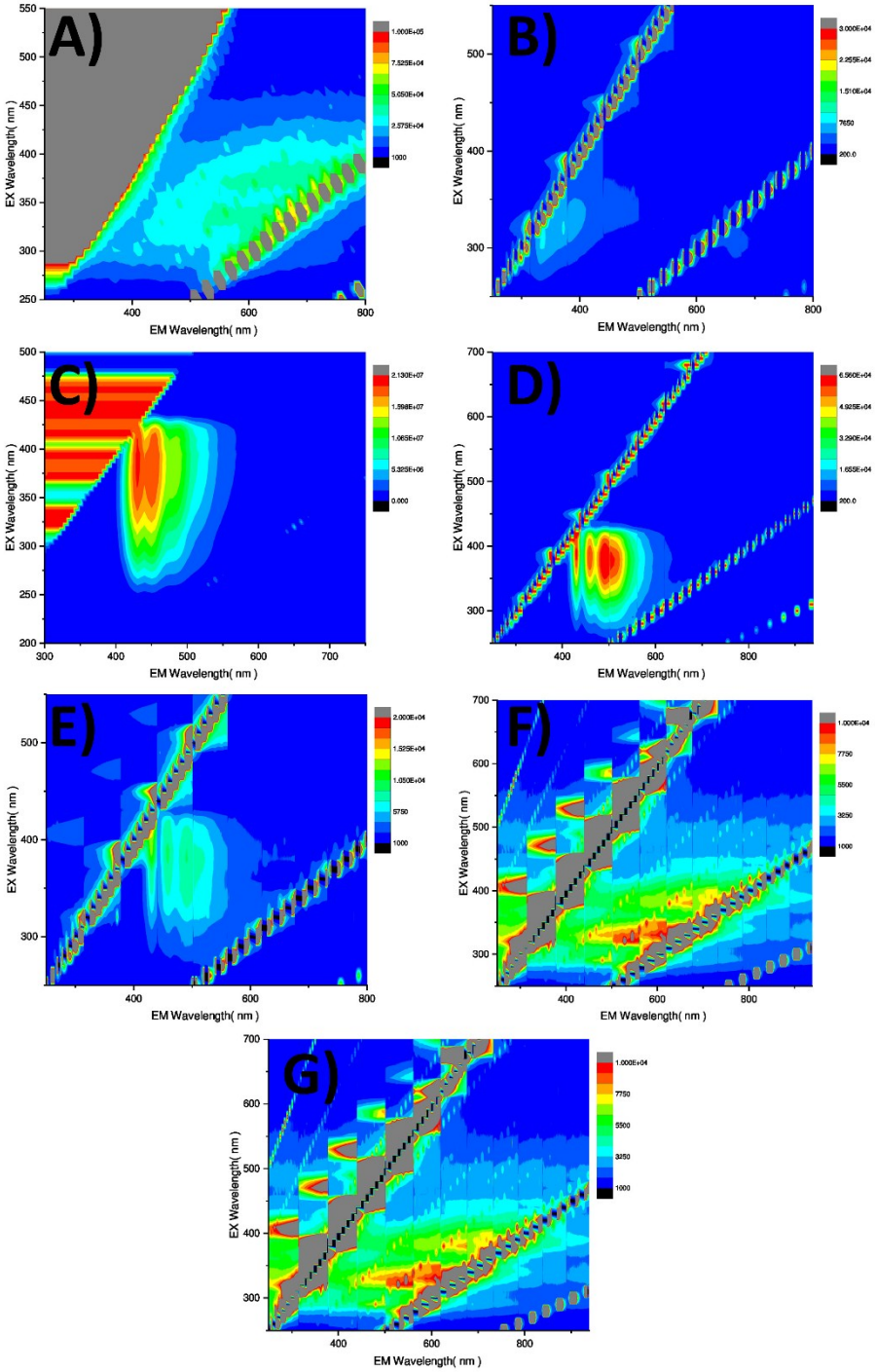

Figure S8. 3D excitation/emission spectra for A) CaGe2 B) Ge_6H_6 C) Ge_4FPh_I D) Ge_4FPh_H E) Ge_4FPh_B F) Ge_Ph_I and G) Ge_Me_I.

XPS spectra

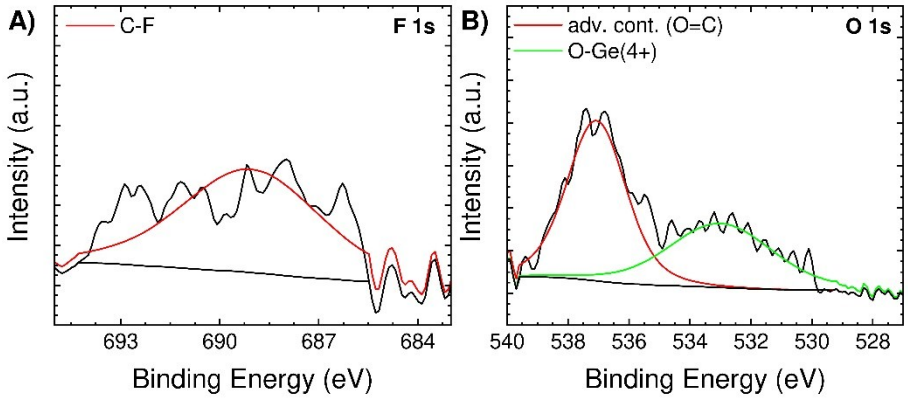

Figure S9. A) F 1s and B) O 1s high resolution XPS spectra for Ge_4FPh_I.

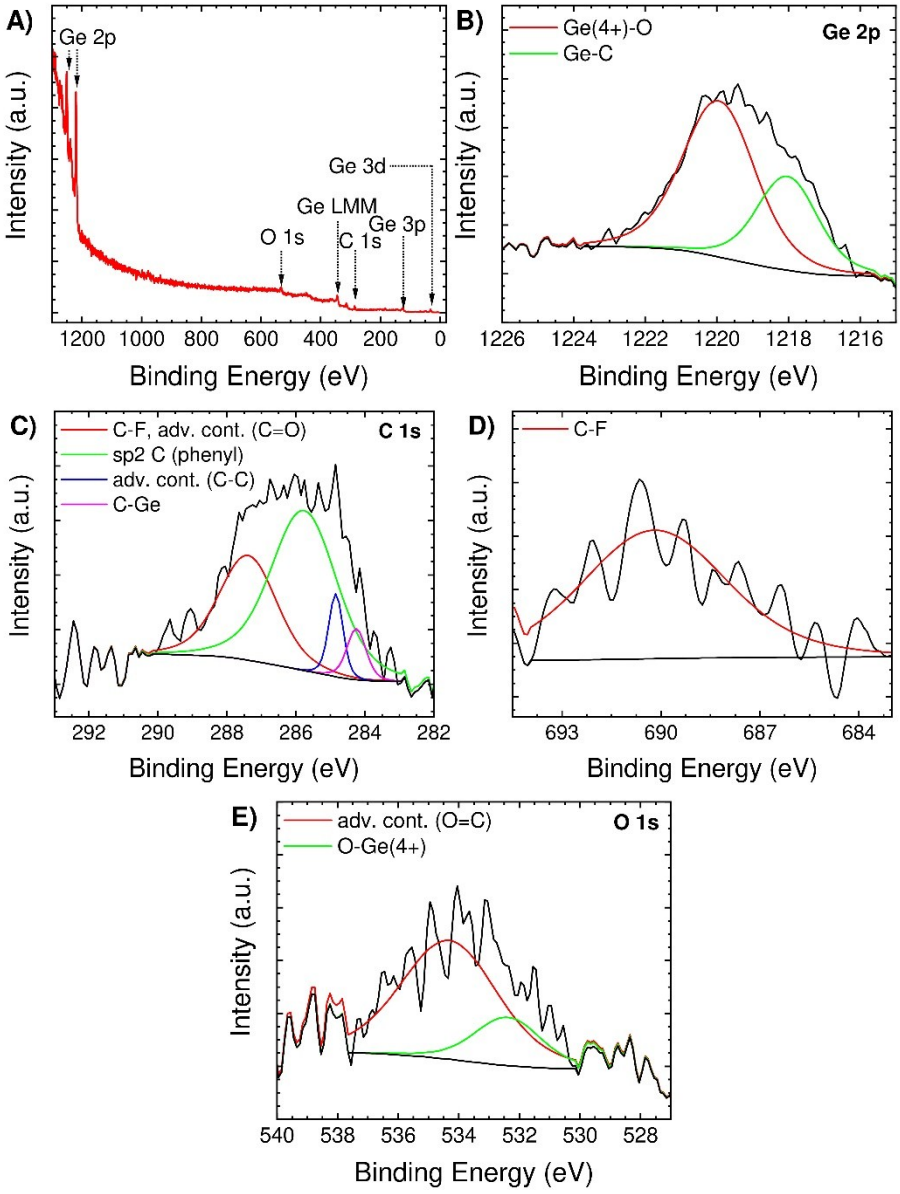

Figure S10. XPS survey spectrum (A) for Ge_4FPh_H and corresponding high resolution spectra: B) Ge $2p_{3/2}$, C) C 1s, D) F 1s and E) O 1s.

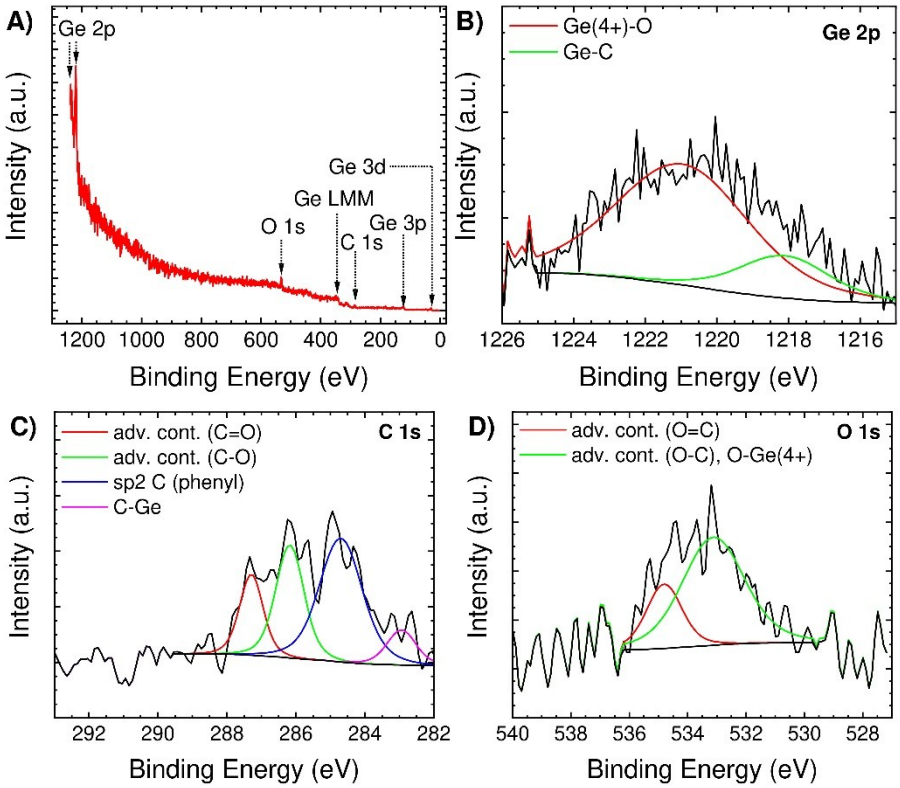

Figure S11. XPS survey spectrum (A) for Ge_4FPh_B and corresponding high resolution spectra: B) Ge $2p_{3/2}$, C) C 1s, D) O 1s.

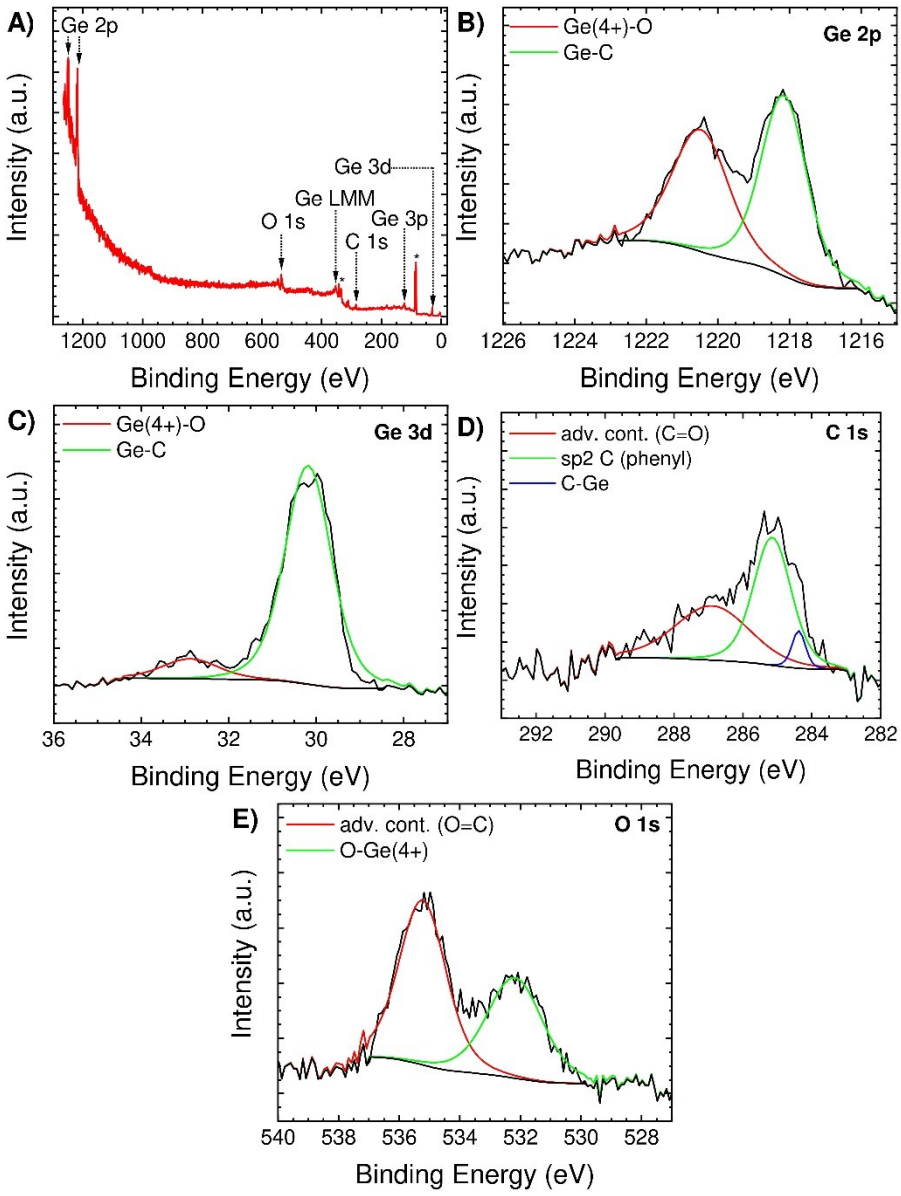

Figure S12. XPS survey spectrum (A) for Ge_Ph_I and corresponding high resolution spectra: B) Ge $2p_{3/2}$, C) Ge 3d, D) C 1s and E) O 1s.

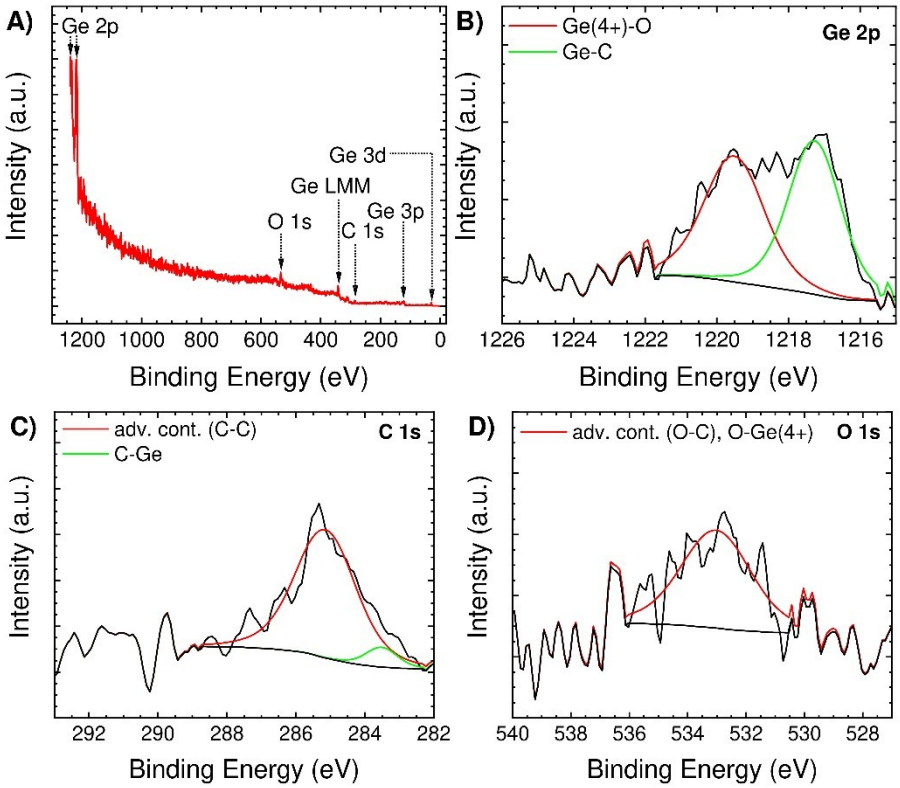

Figure S13. XPS survey spectrum (A) for Ge_Me_I and corresponding high resolution spectra: B) Ge $2p_{3/2}$, C) C 1s and D) O 1s.

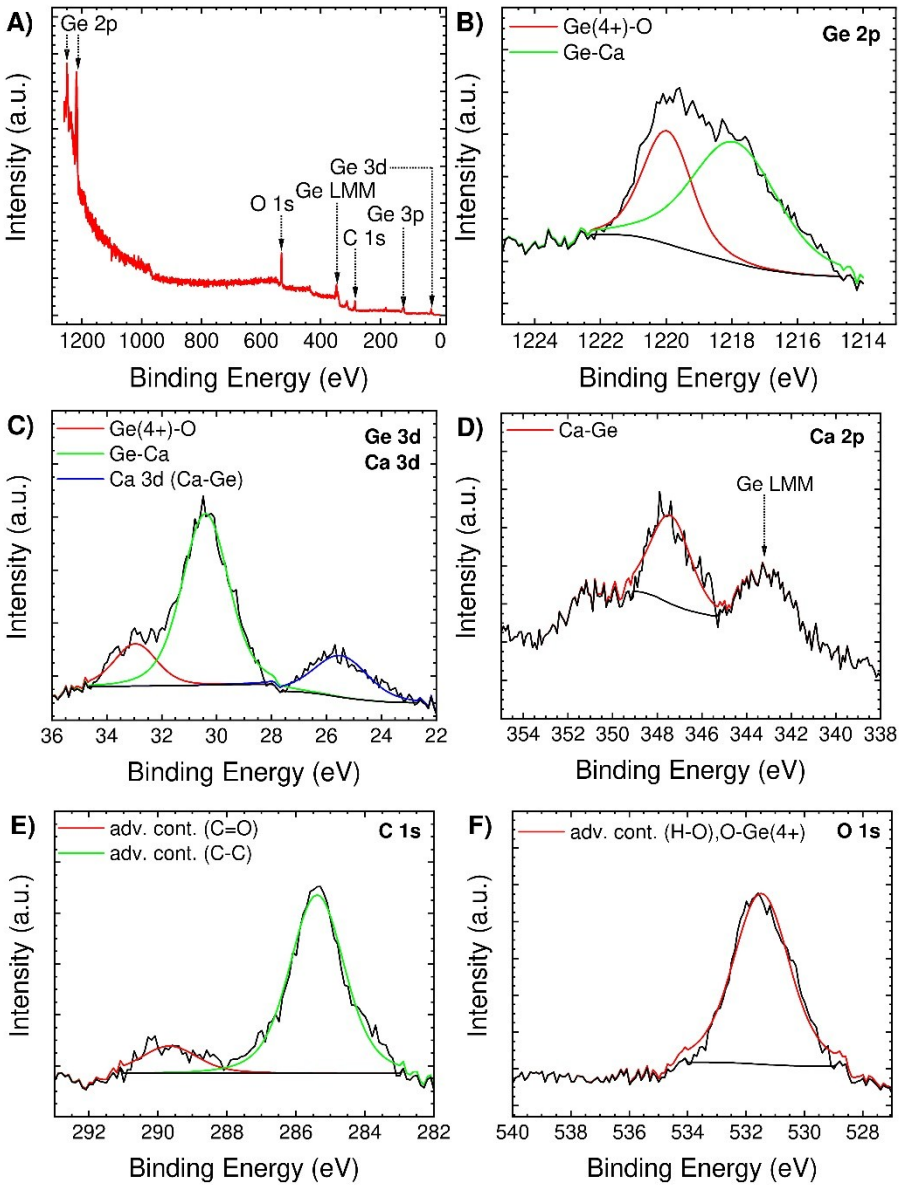

Figure S14. Survey XPS spectrum (A) of $CaGe_2$ and corresponding high resolution spectra for B) Ge 3d + Ca 3d, C) Ge 2p, D) Ca 2p + Ge LMM, E) C 1s and F) O 1s.

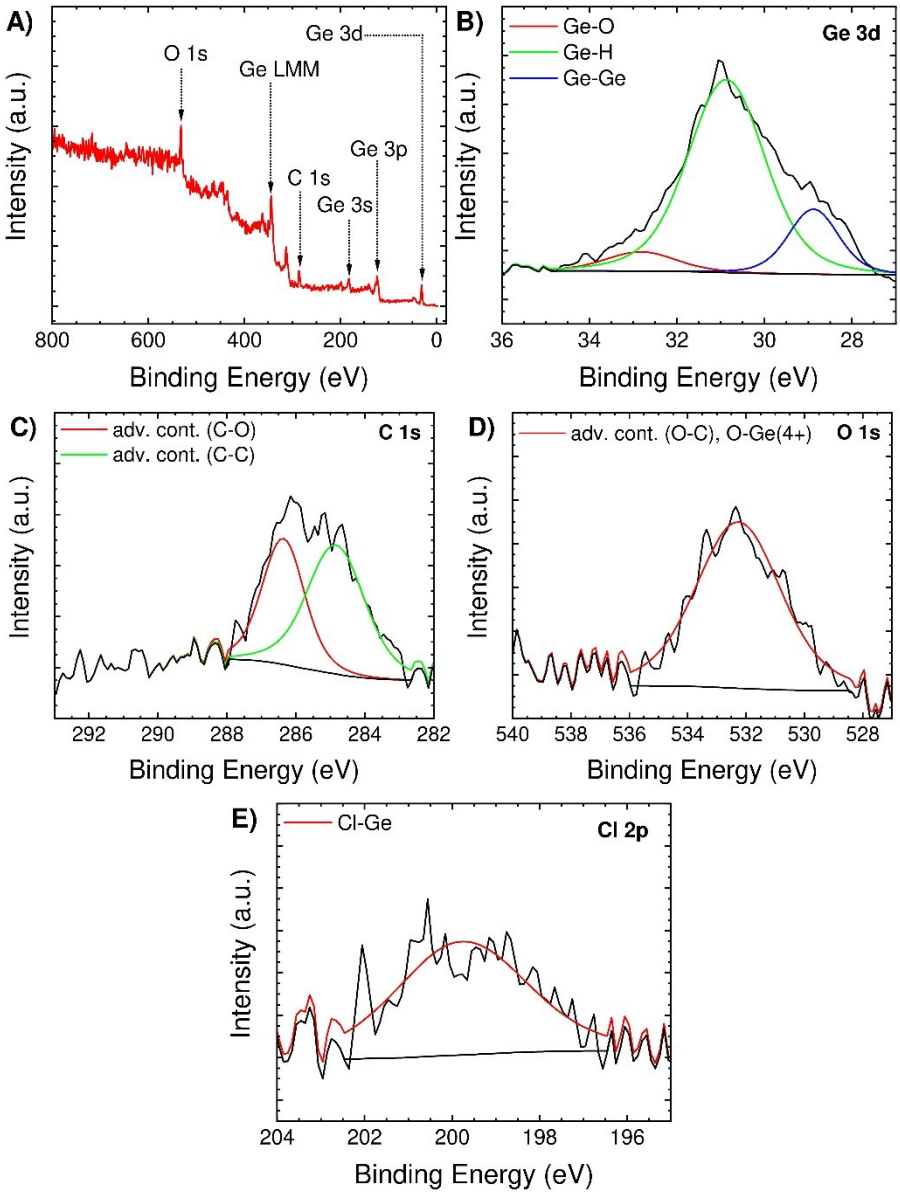

Figure S15. Survey XPS spectrum (A) of Ge_6H_6 and corresponding high resolution spectra for B) Ge 3d, C) C 1s, D) O 1s and E) Cl 2p.

References:

1. Mooney, J.; Kambhampati, P., Get the Basics Right: Jacobian Conversion of Wavelength and Energy Scales for Quantitative Analysis of Emission Spectra. *The Journal of Physical Chemistry Letters* **2013,** *4* (19), 3316-3318.

2. Frisch, M. J.; Trucks, G. W.; Schlegel, H. B.; Scuseria, G. E.; Robb, M. A.; Cheeseman, J. R.; Scalmani, G.; Barone, V.; Petersson, G. A.; Nakatsuji, H.; Li, X.; Caricato, M.; Marenich, A. V.; Bloino, J.; Janesko, B. G.; Gomperts, R.; Mennucci, B.; Hratchian, H. P.; Ortiz, J. V.; Izmaylov, A. F.; Sonnenberg, J. L.; Williams-Young, D.; Ding, F.; Lipparini, F.; Egidi, F.; Goings, J.; Peng, B.; Petrone, A.; Henderson, T.; Ranasinghe, D.; Zakrzewski, V. G.; Gao, J.; Rega, N.; Zheng, G.; Liang, W.; Hada, M.; Ehara, M.; Toyota, K.; Fukuda, R.; Hasegawa, J.; Ishida, M.; Nakajima, T.; Honda, Y.; Kitao, O.; Nakai, H.; Vreven, T.; Throssell, K.; Jr., J. A. M.; Peralta, J. E.; Ogliaro, F.; Bearpark, M. J.; Heyd, J. J.; Brothers, E. N.; Kudin, K. N.; Staroverov, V. N.; Keith, T. A.; Kobayashi, R.; Normand, J.; Raghavachari, K.; Rendell, A. P.; Burant, J. C.; Iyengar, S. S.; Tomasi, J.; Cossi, M.; Millam, J. M.; Klene, M.; Adamo, C.; Cammi, R.; Ochterski, J. W.; Martin, R. L.; Morokuma, K.; Farkas, O.; Foresman, J. B.; Fox, D. J. *Gaussian 16, Revision B.01*, Gaussian, Inc., Wallingford CT, 2016.

3. Yanai, T.; Tew, D. P.; Handy, N. C., A new hybrid exchange–correlation functional using the Coulomb-attenuating method (CAM-B3LYP). *Chem. Phys. Lett.* **2004,** *393* (1–3), 51-57.

4. Grimme, S.; Ehrlich, S.; Goerigk, L., Effect of the damping function in dispersion corrected density functional theory. *Journal of Computational Chemistry* **2011,** *32* (7), 1456-1465.